



Received: 07-11-2025  
Accepted: 17-12-2025

ISSN: 2583-049X

## Superconductors Cuprate Molecular Effect Model Advances with Carnot Factor Graphical Optimization

Dr. F Casesnoves

Independent Bioengineering Laboratory, Registered, Tallinn, Harjumaa, Baltic States, Estonia

Corresponding Author: Dr. F Casesnoves [Email: [casesnoves.research.emailbox@gmail.com](mailto:casesnoves.research.emailbox@gmail.com)]

### Abstract

At previous publication series, the Molecular Effect Model (MEM) with Interior and Graphical Optimization was presented. That study comprised Type I and Type II superconductors materials, both classical and modern ones. This study shows 2D-3D advances in MEM for important Cuprates superconductors and new applications of MEM to

determine-compute Carnot Factor. Imaging-processing in 2D-3D and numerical results with two systems, GNU-Octave and Matlab, are proven and detailed. An improved review of previous contributions in Isotope Effect Interior Optimization for Hg is included. Applications in Electronics Physics Superconductors modelling are explained.

**Keywords:** Molecular Effect M (MEM), Interior Optimization (IO) Methods, Polynomial Fitting (PF), Graphical Optimization (GO), Systems of Nonlinear Equations, Tikhonov Regularization (TR), Inverse Least Squares (ILS), Electronics Superconductors, High-Temperature Superconductors (HTSC), BCS Theory, Carnot Factor (CF)

### 1. Introduction and Objectives

This article continues a series of superconductivity mathematical modelling publications, based on 2D-3D Interior and Graphical Optimization [Refs-8, 1-12]. Today, SC and HTSC constitute a research field/applications framework with quite unpredictable practical/theoretical rapid advances. The Critical Temperature predictions in function of material composition for engineering/manufacturing applications is an important part of the SC and HTSC efficacious usage.

#### 1.1 Fundamental Concepts

The determination of critical temperature ( $T_c$ ) in superconductors Type I and Type II is crucial for power engineering, physics, and industrial applications [Refs-7, 1-9]. The superconductivity research field is an open area whose new advances and applications number is increasing recently. Along a series of articles and a book, [Refs-8, 1-11], 3D Interior Optimization mathematical methods were developed for modelling the classical-exponential BCS equation for classical Type I ( $T_c$ ) determination. Inspired mathematically from Isotope Effect, but with a different modeling technique, the Molecular Effect Model (MEM) for Type II High Temperature Superconductors was primarily built up. In that research line, 2D-3D Interior and Graphical Optimization modeling-methods were applied for MEM in cuprates, Example-Figure 1.

Therefore, this new contribution presents advances for MEM model in HTSC cuprates, one of the most important families in HTSC. In addition, the practical Carnot Factor, [Refs-7, 1-2], applied on superconductivity for cuprates, is optimized in 2D-3D imaging-processing and numerical data.

Results comprise a database of BCS and MEM ( $T_c$ ) values for Type I and Type II superconductors. The challenges for future SC and HTSC research are described in Table 1, [Casesnoves, 2021, author's proposal]. Then, some views in this field for the future superconductivity advances are also included Tables 1-2, [Refs-9, 49]. Consequently, the article has two main strands. Namely, the improvements for MEM in HTSC cuprates, and Carnot Factor 2D-3D Graphical Optimization. Additionally, an extended/complemented review of Hg Isotope Effect, 2D-3D Graphical/Interior Optimization, set in simplified concepts/graphs, is presented. Future trends and research lines/areas for HTSC are shown in Tables 1-2. Engineering and Physics applications are briefed.

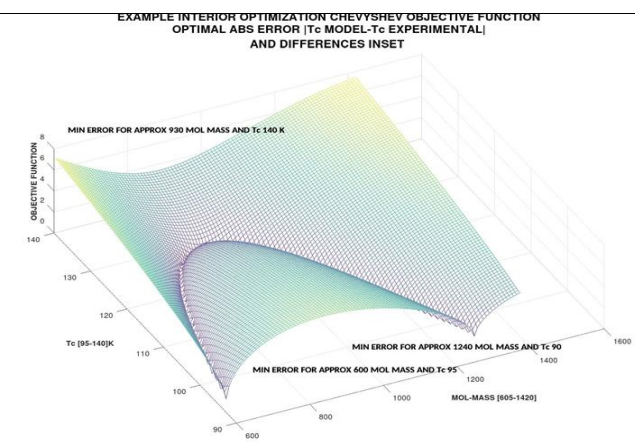
**Table 1:** Improved-modified from a previous conference publication, [Refs-8, 11], Author's proposal about future superconductivity, strategic research lines according Overview of possible future developments/applications for SC and HTSC applications in transmission lines

SUPERCONDUCTORS POWER-ENGINEERING FUTURE CHALLENGES [ Author's Proposal ]			
Overview Type	Advance	Limitation	Additional
Copper and classical line transmissions. For example: single triaxial HTS cable operating at 13 K with carrying 69 MVA of power [Refs-9, 49].	Substitution of classical transmission lines (TL) with savings of common metal materials.	Length of TL. And materials/energy cost for cooling superconductors.	The new Type II HTSC might overcome some or several of those technical hurdles.
Classical line transmission substitution. Superconductivity in the Future Electric Grid for short-distances.	Increase of savings in space and underground conduction space. Reduce electricity costs through intracontinental power marketing. Specially power engineering super-computer demands.	According to ground, land, urban surroundings, safety conditions, etc. However refrigeration issues make long distances connections difficult.	Cost of staff, designers, refrigeration technology, additional power-plant engineering changes derived of the new system.
High-Voltage Transmission Lines.	Theoretical projects advances. From [Refs-9, 49]: "within the superconducting layers of the new SC superconductors, current densities are typically more than 10,000 times higher than those possible in copper".	Several, as High-Voltage TL are much longer and transmit high-power energy. High magnetic field that should be shielded.	The more progress in new SC and HTSC materials, the better possibility. The magnetic field is reduced since one HTSC TL takes less volume-space. Reduction thermal and electromagnetic contamination field (EMF) for population surrounding underground infrastructure.
Energy efficiency and loss savings.	Theoretically extremely high savings and efficiency. Conventional transformers replacement. [Refs-9, 49]. Function optimization to substitute the necessary conventional transformers exclusively. Then, from [Refs-9, 49], significant energy losses occur in conventional transformers as a result of the iron in the cores (load losses) and the copper in the windings (load losses).	Limited by construction costs, cooling devices, underground construction, etc. Conversion technology phases could result in high cost.	The more progress in new SC and HTSC materials, the better efficacy in savings possibilities.
Intense magnetic Field generated surrounding neighborhood. Magnetoradioprotection problem.	How can be taken advantage of this magnetic field and at the same time avoid magnetoradioprotection risks? .	Explore this engineering energy approach possibility. Resulting magnetic energy could be extracted? .	The magnetic field generated by SC is intense. Shielding is necessary at some places. For example electromagnetic damage possible to vulnerable surrounding people etc.

**Table 2:** From a previous conference publication, [Refs-8, 11] future strategic research lines according [Refs-9, 49, Sarrao, J; Nault, R. (2006). This is a briefing of future investigation areas. Those are basic research needs for superconductivity] criteria.

Note: that is an overview and brief resume with data of a prestigious institution among other conferences about SC and HTSC research institutes

SUPERCONDUCTORS POWER-ENGINEERING AND ELECTRONICS SOME FUTURE STRATEGIC RESEARCH LINES	
[ From 49, Sarrao, J; Nault, R. (2006). Basic research needs for superconductivity.]	
PRIORITY	REASONS AND OBJECTIVES
[ Directly From 49, Sarrao, J; Nault, R. (2006)]	
Identifying simplified criteria for screening materials and implementing them into Computational Algorithms	Elaboration of screens for new-potential superconductors will enable this search, because it will allow identification of the most likely materials with faster/slower conductivity. Then, substitution of classical SC with more reliable and operational ones.
Integrating Synthesis and Surface-Sensitive Characterization Techniques	There are new laboratory techniques to be used for these objectives, such as molecular beam epitaxy (MBE), applicable for films of various complex oxides.
Computational Libraries of Potential Superconductors	Efficient and efficient techniques/methods for creating materials libraries that could be used for new properties.
Developing Reliable and Fast Methods to Determine the Surface Structure	This is an important point as it saves laboratory time for characterization of potential new superconductors, and therefore increases probabilities of advances.
Enabling materials for superconductor utilization	Materials apparently unable to show superconducting properties could get that characteristics by using modifications.
Low-temperature Insulators	Insulators are essential to reach optimal critical temperatures. That involves both mechanical improvements and thermal properties research.
Magnets and Dielectrics	More efficient and efficient transformers for more optimal magnetic fields and capacitors.
Control Systems	For example, MOSFETs, capacitors, inductors with better cryogenic properties given by new materials.
Maximize Refrigeration Efficiency	That is a field of convergence for several branches, namely, Chemistry, Mechanics, Thermodynamics and Thermo-Physics.



Example-Figure 1.- Molecular Effective Model got for Cuprates with minimum error. For example, inset, according to Table 3, [Abs-Error  $\leq$  8 K] for approx [605, 1420] molecular mass and Tc around [95,140] K. That is, the approximation of MEM matches published experimental Tc [Refs-7, 1,2]. Note that in this tentative program imaging-processing the surface graphical optimization is rather complicated but fits approximately experimental results. Observe the shape similarities between the 3D surface parabolic geodesics and the 2D parabolic curves of Figure 1. The Table 3 Cuprates shows a parabolic-numerical-shape with approximately the same Tc for low molecular masses, and high ones, while for intermediate molecular mass magnitudes the Tc values are the highest. Just that is proven at this MEM computational-graphical optimization.

## 1.2 Research Objectives

Research objectives are mainly two. The first one is to improve the Molecular Effect Model for cuprate HTSC from previous publications, [Refs-8, 1-13]. Secondly, to begin the study of Carnot factor for HTSC by using MEM models. Complementary and illustrative, to review the precision obtained with Interior Optimization Method for Hg, which is useful as Hg is a chemical element whose isotopes show a varied statistical composition in this natural element, [Refs-7, 1-3]. Applications for HTSC electronics physics are briefed.

*Grosso modo*, this article shows improvements for Molecular effect Model for cuprates and findings for 2D-3D Graphical optimization cuprates Carnot Factor. Complementary an improved review of Hg Isotope Effect and electronics physics applications are detailed.

## 2. Mathematical and Computational Methods

The programming techniques are related to previous research [Refs-8, 1-9, Refs-8, 19-23] and dual-program design [Refs-8, 9-10]. Along those articles, software and 2D-3D imaging processing details with explanations are included. With the 2D polynomial fit data, it is possible to get approximations for further setting of Genetic Algorithms constraints and lower/upper boundaries, but that is not the study objective.

### 2.1 Interior Optimization

Interior Optimization is a method, [Refs-8, 1-9], that was developed computationally mainly for electronics physics applications, although is a mathematical-computational general method. Specifically was published, [Refs-8, 9], for Isotope Effect in several SC elements. Here was used for getting the best polynomial algorithm in the selected, Table 3, HTSC cuprates.

### 2.2 Graphical Optimization

Graphical Optimization method was developed by Author in 2016, mainly for metal hardness mathematical modelling, [Refs-9, 12]. Later on, in publication series for several research areas, [Refs-8, 1-10, Refs-9, 21]. Basically, this method involves the numerical fit of the objective function set in a 3D surface to find with precision the global, local, partial, desired-selected, or approximated minima. Here it is used to get the accurate difference in Kelvin degrees between Tc experimental, Table 3, and Tc of the model, results at Table 4. Note that since the 2D and 3D imaging-processing charts, Figures 1-4, give a large numerical values

at prompt, it is possible guess the prediction of  $T_c$  for a different cuprate compound whose isotope composition makes difference from the standard experimental dataset, Table 3. That is in fact the objective-usage of the present study here.

### 2.3 HTSC Cuprates Computational Dataset

There are several Cuprates HTSC major families [Refs-7, 1,3]. Namely, Hg-Ba-Ca-Cu (the subject of this study), Thallium-based cuprates, those compounds formed when Tl is substituted by Bi or when Ba is replaced by Sr, and some of them with Rare Earths. This study is based on Hg-Ba-Ca-Cu-O compounds/family, as it is widely used in industry, Table 3. In that data-table HTSC cuprates show a parabolic-shape distribution with approximately the same  $T_c$ , Example Figure 1, for low molecular masses, and high ones. Instead, for intermediate places molecular mass magnitudes for corresponding  $T_c$  values are the highest, Figure 1, Table 3. In such a way, the relative-numerical links among molecular masses and  $T_c$  was used for creating the Molecular Effect Model. It is inspired from classical Isotope Effect one [Refs-7, 1-3, Refs-8, 1-3, 9-10]. Hg-Cuprate compounds show a very useful/practical  $T_c$ , and as an instance, it is about the night temperature of the moon, [Refs-7, 9].

**Table 3:** Software programming selected data with references for Cuprates Hg-Ba-Ca-Cu-O group [Refs-7, 1-3]. The criterion for ordering data was increasing molecular mass. Details are included

CUPRATES COMPUTATIONAL SOFTWARE DATASET [Mainly from Hott et al., 2005; and Superconductors.org, 2025 ; Tetragonal Crystal Lattice]			
Cuprate Type	Molecular Weight	$T_c$ [Kelvin, K]	Additional
HgBa <sub>2</sub> Ca <sub>6</sub> Cu <sub>7</sub> O <sub>16</sub>	1416.5400	88	Minimum $T_c$
HgBa <sub>2</sub> Ca <sub>5</sub> Cu <sub>6</sub> O <sub>15</sub>	1312.8960	107	Decreasing $T_c$
HgBa <sub>2</sub> Ca <sub>5</sub> Cu <sub>6</sub> O <sub>14</sub>	1280.9000	97	Decreasing $T_c$
Hg <sub>2</sub> Ba <sub>2</sub> Ca <sub>3</sub> Cu <sub>4</sub> O <sub>12</sub>	1242.2420	114	Decreasing $T_c$
HgBa <sub>2</sub> Ca <sub>4</sub> Cu <sub>5</sub> O <sub>13</sub>	1161.2750	110	Decreasing $T_c$
Hg Ba <sub>2</sub> Ca <sub>4</sub> Cu <sub>5</sub> O <sub>12</sub>	1145.3000	110	Decreasing $T_c$
(Hg <sub>0.8</sub> Tl <sub>0.2</sub> )Ba <sub>2</sub> Ca <sub>2</sub> Cu <sub>3</sub> O <sub>8.33</sub>	1096.1000	138	Maximum $T_c$
HgBa <sub>2</sub> Ca <sub>3</sub> Cu <sub>4</sub> O <sub>11</sub>	1025.6530	127	Increasing $T_c$
Hg Ba <sub>2</sub> Ca <sub>3</sub> Cu <sub>4</sub> O <sub>10</sub>	1009.7000	125-126	Double point for optimization
Hg <sub>2</sub> Ba <sub>2</sub> Ca <sub>2</sub> Cu <sub>3</sub> O <sub>10</sub>	1106.6000	45	N/A, $T_c$ difference too high
Hg <sub>2</sub> Ba <sub>2</sub> CaCu <sub>2</sub> O <sub>8</sub>	971.0000	44	N/A, $T_c$ difference too high
HgBa <sub>2</sub> Ca <sub>2</sub> Cu <sub>3</sub> O <sub>9</sub>	890.0300	134	Increasing $T_c$ but low Molecular Mass
Hg Ba <sub>2</sub> Ca <sub>2</sub> Cu <sub>3</sub> O <sub>8</sub>	874.0432	133-135	Double point for optimization
HgBa <sub>1.8</sub> Tl <sub>0.2</sub> Ca <sub>2</sub> Cu <sub>3</sub> O <sub>10</sub>	804.6400	138	Increasing $T_c$
HgBa <sub>2</sub> CaCu <sub>2</sub> O <sub>7</sub>	754.4100	128	Increasing $T_c$
Hg Ba <sub>2</sub> CaCu <sub>2</sub> O <sub>6</sub>	738.4200	126	Increasing $T_c$
HgBa <sub>2</sub> (Ca <sub>1-x</sub> Sr <sub>x</sub> )Cu <sub>2</sub> O <sub>6+</sub>	738.4100	123-125	For (x=0), Double point for optimization
HgBa <sub>2</sub> Cu <sub>1</sub> O <sub>5</sub>	618.7900	97	Approximated Minimum $T_c$
Hg Ba <sub>2</sub> Cu O <sub>4</sub>	602.7936	97	Approximated Minimum $T_c$

### 2.4 Carnot Factor Optimization

Carnot Factor (CF), is commonly used to optimize the industrial cost of superconductivity usage [Refs-7, 1,8,9]. It is based on the classical Carnot Cycle in Thermodynamic Physics. For refrigerator cycles, there is a large variety of thermodynamical ones, [Refs-7, 9]. Most applied theoretical cycles are the Carnot and Claude cycles, however the options are varied. The refrigerator whether liquid or gas constitutes an essential part of the cooling system. A classical refrigerator was liquid nitrogen, [77 K], [Refs-

7,1,8,9]. Recently, [e.g., 2016, Refs-7, 8] most applied for superconducting lines are liquid hydrogen ( $T_c = 20$  K), liquid nitrogen, [77 K], liquid helium for Low Temperatures Superconductors [ $T = 4.2$  K]. For superconductivity below [ $T = 39$  K], [Refs-7, 8], both helium gas or liquid nitrogen.

Therefore, today Carnot Factor for thermodynamical efficiency continues being used effectively. In general, at [ $T = 4.2$  K], the superconducting energy has not an economically optimal cost [Refs-7, 1]. The so-called Operation Temperature is fundamental parameter for Carnot Factor determination. An example is shown at [Refs-7, 1], namely '*to remove a heat input of 1 W an ideal, reversible refrigerator consumes at room temperature a power of 70 W for Top = 4.2 K, whereas this power is only 2.9 W for operation at 77 K*'. Critical current is another important constraint for the economic cost of superconductor devices, but not the focus of this study, [Refs-7, 1].

In brief, the second objective of this research is to optimize in 2D-3D the CF for HTSC cuprates of Table 3. Hence the CF algorithm, [Refs-7, 1], reads,

$$\text{Carnot Factor (CF) Fundamental Equation, } CF = \frac{300 \text{ K} - T_{\text{operating}}}{T_{\text{operating}}}; \quad (1)$$

Where,

CF: Carnot Factor (adimensional).

K: Kelvin.

$T_{\text{cold}} = 300$  K (usually). Note that in Figures 5-8, it is set at programs in intervals [275,326].

$T_{\text{operating}}$ : Operating temperature of the superconductor device (K) [Refs-7, 1]. In Figures-software is set at [20,120] or [0,120] K.

This formula is applied for 2D-3D numerical determinations in two ways. In 2D, first one is setting a range of  $T_{\text{operation}}$  interval [0, 120] K, and at the second, but computationally more difficult, implementing simultaneously a  $T_{\text{cold}}$  interval of [275, 325], Figure 5. Just the same second method was used for 3D CF surface, Figures 5-8.

### 3. 2D-3D Graphical-Interior Optimization and Numerical Results

Based on Subsections 2.2 and 2.3, the software-programming results for these methods, graphical and numerical, are demonstrated /shown in the following, Figures 1-8,Table 4.

#### 3.1 2D-3D Graphical Cuprate MEM Optimization

The graphical-interior simulations in 2D-3D are done by using and improving previous publications superconductivity software, [Refs-9, 1-10], mainly. According to Example Figure 1, the first step is to order database of Table 3 for programming. After that, a regression polynomial fit is designed in four phases to obtain a final continuous 3-degree optimal polynomial of  $T_c$  in function of the molecular mass, Figure 1. It was found no significant numerical precision difference between a 3-degrees and a 4-degrees fit. The initial polynomial equation is set with further software to obtain a continuous model, through these successive steps, Figure 1, Equation (2). Both GNU-Octave and Matlab systems were/could be used for 2D-3D graphics, and in most of cases programs are equivalent with few differences, Figures 1-4. Proven Molecular Effect Model: The parabolic shape of Figure 1 is

extrapolated to Figure 2, inset, red polygon, and model efficacy is demonstrated.

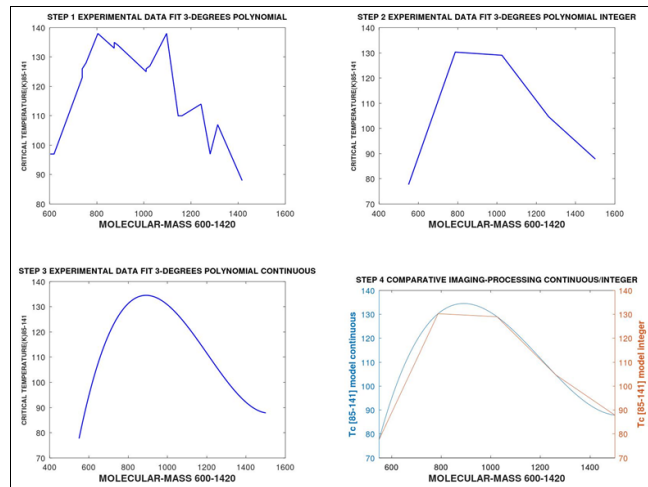


**Fig 1:** GNU-Octave 2D Molecular Effective Model for Cuprates programming-construction with minimum error, four stages. As in Example Figure 1, these 2D approximations of MEM match published experimental  $T_c$  [Refs-7, 1-3], Table 3. From step 1 to step 4, it is demonstrated the efficacy of the polynomial fit, Equation (2). Note in this tentative program imaging-processing that the geodesic surface of Example Figure 1 indeed contains/shows these curves or integer approximations. Every curve shape from step 1 to step 4 has a different fitting software, and to obtain those stage by stage is rather complicated/laborious. The Table 3 Cuprates shows a parabolic-shape with approximately the same  $T_c$  for low molecular masses, and high ones, while for intermediate molecular mass magnitudes the  $T_c$  values are the highest. Just that is proven at this 2D MEM computational-graphical optimization. Matlab programs for this 2D imaging-processing are almost equivalent. Next Figure 2 demonstrates these parabolic shapes reproduced with precision at 3D MEM model

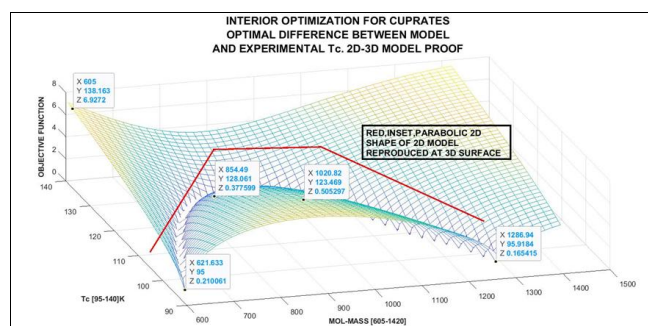


**Fig 2:** Matlab 3D Molecular Effective Model for Cuprates with minimum error, marked inset numerical data. As in Example Figure 1, those 2D approximations of MEM match published experimental  $T_c$ . A polygon resembling the parabolic shape of the Figure 1, (inset, in red), shows the geodesic similarities with 2D curves of Figure 1. Note the low absolute errors (Z values) got with the polynomial MEM model, Equation (2). The matrices software to obtain this image-processing is rather difficult, not for program length, but for matrices congruence

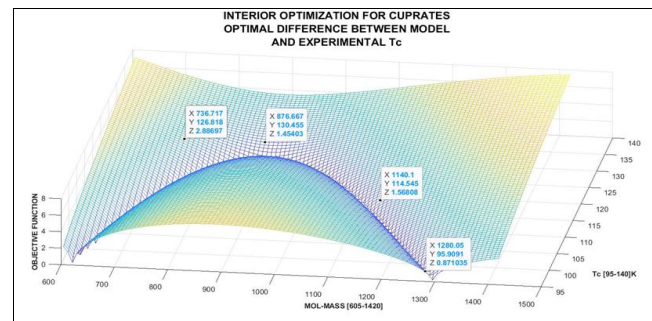


**Fig 2.1:** Matlab 3D Molecular Effective Model for Cuprates with Table 4 extracted dataset. It is intended to prove the absolute error improvements for the MEM model. Absolute error, according to this image and Table 4, is: 2D-3D abs errors (K);  $[0 \leq \text{Abs Error} \leq 8]$  (K). Marked inset, numerical data. As in Example Figure 1, those 2D approximations of MEM match published experimental  $T_c$ . Note more clearly the low absolute errors (Z values) got with the polynomial MEM model, Equation (2). As in Figure 2, the matrices software to obtain this image-processing is rather difficult, not for program length, but for matrices congruence

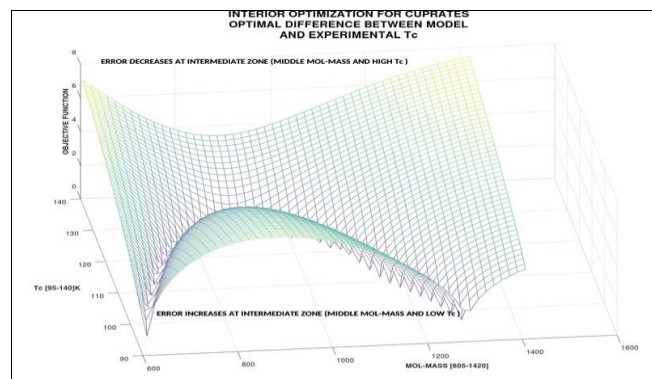


**Fig 3:** GNU-Octave 3D Molecular Effective Model for Cuprates with Table 3 extracted dataset. It is intended to show the absolute error improvements and error distribution along the surface (Notes inset). Absolute error, decreases at posterior surface part, and increases at anterior one. According to this image and Table 4, is: 2D-3D abs errors (K);  $[0 \leq \text{Abs Error} \leq 8]$  (K). As in Matlab imaging-processing Figures 2, 2.1 the matrices software to obtain this image-processing is rather difficult, not for program length, but for matrices congruence. The GNU-Octave image processing quality is acceptable but Matlab is better

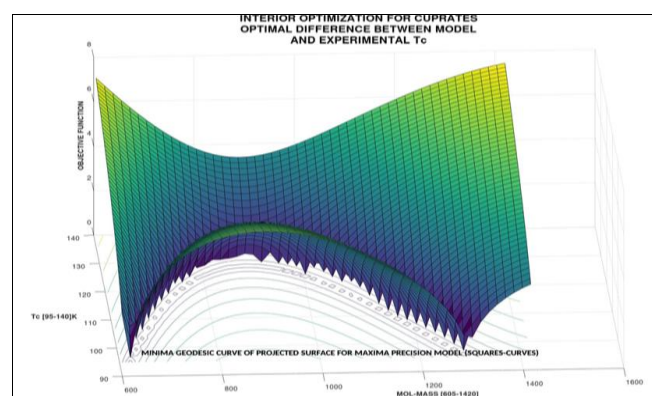


**Fig 4:** This GNU-Octave image was programmed for showing clearly the geodesic error projections and surface curves marking the minima (squares or small polygons) curve from where the surface begins to get higher Z-coordinates at the posterior. That is, the minima geodesic projections where the surface begins to grow towards posterior and anterior directions are shown with those small squares. The image-processing subroutine at pattern is different from Figure 3

### 3.2 2D-3D Graphical Cuprate Carnot Factor (CF) Optimization

According to Equation (1), CF constitutes a practical numerical reference for functional manufacturing and operating of SC and HTSC devices. Figure 5 was designed with 2D software-engineering inspired in [Refs-7, 1], but with variable intervals for both  $T_{\text{operation}}$  and  $T_{\text{cold}}$  (blue for fixed  $T_{\text{cold}}$  at 300 K, and red-dashed or black for variable intervals of  $T_{\text{operation}}$  and  $T_{\text{cold}}$ ). It is proven that, even separating the curves (second chart right,  $x+10, y+10$ ), the shapes are almost coincident. That is corroborated at 3D implementation, Figures 6-8.

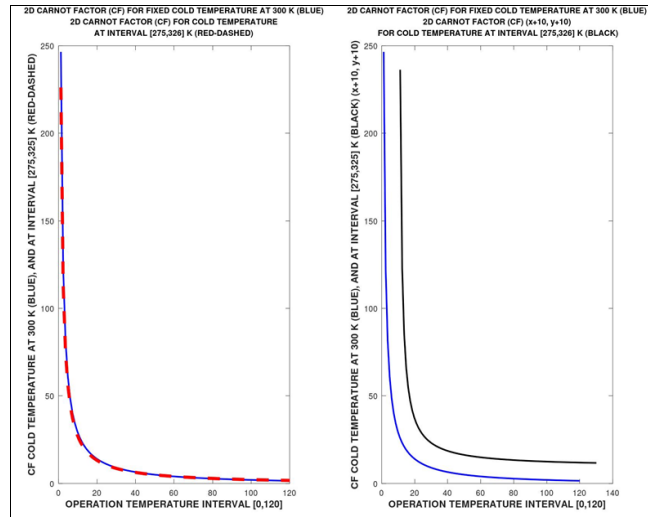


**Fig 5:** GNU-Octave 2D Carnot Factor for Cuprates with two programming techniques. Matlab programs for this 2D imaging-processing are almost equivalent. Red dashed-line, inset left, shows variable intervals for both  $T_{\text{operation}}$  [0,120] K, and  $T_{\text{cold}}$  fixed at 300 K, while the blue coincident line correspond to CF with  $T_{\text{cold}}$  [275,326] and  $T_{\text{operation}}$  [0,120]. At right, both curves are separated to prove almost total coincidence, that is, blue curve is for fixed  $T_{\text{cold}}$  at 300 K, and black one shows CF for  $T_{\text{cold}}$  interval [275,326]. For better visualization, the second methods, inset black, shows a small translation (second black curve,  $x+10, y+10$ ), the shapes are almost coincident

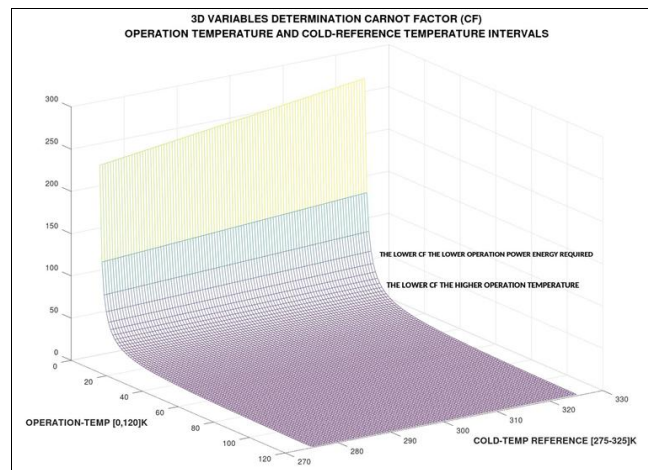


**Fig 6:** GNU-Octave 3D Carnot Factor model for Cuprates with  $T_{\text{cold}}$  interval [275,325] and  $T_{\text{cold}}$  one [0,120]. minimum error. Marked inset, the variable gradients. In other words, the lower CF, the lower operation power energy required. Besides, the lower CF, the higher operation temperature

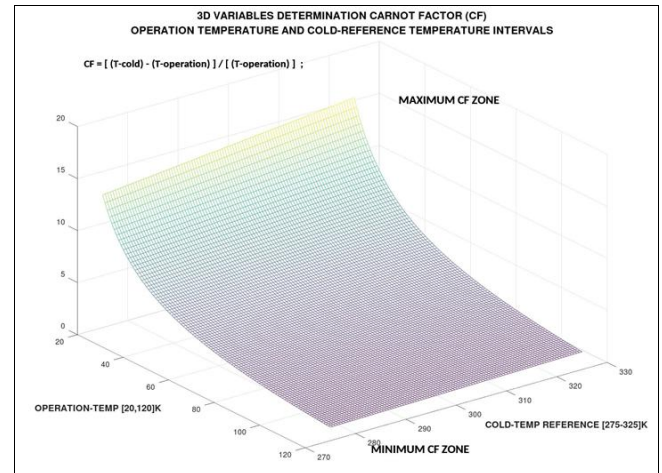


**Fig 7:** GNU-Octave 3D Carnot Factor model for Cuprates with  $T_{\text{cold}}$  interval [275,325] and  $T_{\text{cold}}$  one [0,120]. minimum error. Marked inset, the minimum CF zone, and the maximum Cf area. Matrices at program patterns have to be calculated precisely

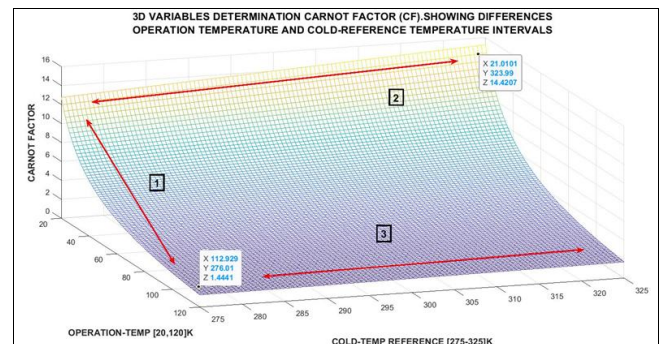


**Fig 8:** Matlab 3D Carnot Factor model for Cuprates with  $T_{\text{cold}}$  interval [275,325] and  $T_{\text{cold}}$  one [0,120]. minimum error. Marked inset with red-lines directions, the variable gradients. The lower CF, the lower operation power energy required. Besides, the lower CF, the higher operation temperature. Some numerical data are shown for illustration. Direction (1) proves the lower CF, the higher operation temperature at low  $T_{\text{cold}}$  (about 275 K). Direction (2) shows the higher  $T_{\text{cold}}$ , the higher CF, at low  $T_{\text{operation}}$  (about 20 K). Direction (3) proves the higher  $T_{\text{cold}}$ , the higher smoothly CF, at high  $T_{\text{operation}}$  (about 120 K)

### 3.3 Numerical Results

The numerical results have two strands. The first one is the MEM model equation that was used for  $T_c$  predictions in function of cuprates HTSC molecular mass. That is, the main algorithm since some variants were applied in specific programs. The second is the comparative numerical results that can be got from the Matlab and GNU-Octave 2D-3D plots. In Matlab it is easier and the cursor at prompt/display can give more numerical information. Table 4 shows some numerical-comparative results. The main algorithm obtained by polynomial fit reads,

$$\text{The Critical Temperature, } T_C(M), \text{ for Cuprates Molecular Effect Model, } T_C = (3.81690545423224e - 07) M^3 + (-1.378534024981543e - 03) M^2 + (1.547508999519298) M + (-4.198839134235919) 10^2 - (420.980091430742)^{0.46}; \quad (2)$$

Where,

$T_c$  (M): Function of Critical Temperature ( $T_c$ ) as function of Cuprates Molecular Mass (M) from Table 3 dataset polynomial optimization.

**Table 4:** 2D-3D Cuprates MEM model with errors according to Figures 1-4. Absolute Error is  $[0 \leq \text{Abs Error} \leq 8]$  (K). Average 2D-3D Error= 4.0633 K; (Figures 1-4). Results are improved from previous publications [Refs-8, 1-13]

NUMERICAL RESULTS AND ERRORS			
<b>Graphical-Optimization Method for Error Boundaries Calculations:</b> From 2D-3D model curves and surfaces. Figures, 1-5, the magnitude values of Table 3 are tentatively sought with GNU-Octave (2D) and Matlab (3D) cursors. Then, the figures given by the 2D and 3D dataset are used to calculate tentatively the maximum and minimum errors among the experimental $T_c$ and the model $T_c$ . The highest differences between Table 3 experimental data and model values are taken to determine the global error boundaries. The final calculation is done with a simple Matlab or GNU-Octave program.			
<b>3D NUMERICAL RESULTS, EXAMPLES</b>			
MOLECULAR MASS EXPERIMENTAL [APPROXIMATED TO Table 3]	$T_c$ EXPERIMENTAL (K) [Table 3]	$T_c$ MOLECULAR EFFECT MODEL CONTINUOUS MODEL PREDICTION (K) [Figure 2.1]	3D ABS ERROR (K) : $[0 \leq \text{Abs Error} \leq 8]$ (K) Average 3D Error= 4.0633 K ; (Figures 2-4) [ Although some errors are high, the statistical mode is low, then average error results be about 4 K ]
736.7170	123-125	126.8180	~ 0
876.6670	133-135	130.455	~ 0
1140.1000	110	114.5450	1.57
1280.0500	97	95.9091	0.87
<b>2D NUMERICAL RESULTS, EXAMPLES</b>			
MOLECULAR MASS EXPERIMENTAL [Table 3]	$T_c$ EXPERIMENTAL (K) [Table 3]	$T_c$ MOLECULAR EFFECT MODEL CONTINUOUS MODEL PREDICTION (K) [Figure 1]	2D ABS ERROR (K) : $[0 \leq \text{Abs Error} \leq 8]$ (K) Average 2D Error= 4.0633 K ; (Figure, from step 3-4) [ Although some errors are high, the statistical mode is low, then average error results be about 4 K ]
602.7936	97	95.93	1.07
738.4100	123-125	124.34	~ 0
874.0432	133-135	134.68	~ 0
1025.6530	127	129.04	2.04
1241.2420	114	106.73	7.27
1280.9000	97	101.04	4.04
1416.5400	88	91.00	3.00

#### 4. Briefing-Review of Hg Isotope Effect Interior Optimization

This is a review about the fundamentals of Interior Optimization Method [Refs-8, 9, text-paragraphs and some images], focused on first chapters of [Refs-8, 9,13], and the initial invention articles, [Refs-8, 1-2]. In plain language, Interior Optimization is a numerical computational-graphical method based on graphical variables separation techniques, which are applied in subsequent 3D imaging stages, which could be also 2D. That is, the analytical partial differential equations method basis is used to make a graphical-optimal numerical determination-selection through 3D/2D imaging-stages in order to select the best/desired values of any several variables algorithm. In this briefing, the mathematical and computational fundamentals of the method are shown with Hg Isotope Effect results. Initially, these techniques were designed for superconductor modelling optimization, specifically BCS Isotope Effect optimization, the Molecular Effect Model (MEM), and Superconducting Multifunctional Transmission Lines Project [Refs-8, 9, 12,13]. All these optimization approaches can be utilized for any science branch that could demand this necessary type of mathematical-computational methods. Interior Optimization Method is defined as follows,

**Definition I:** Interior-Graphical Optimization Method, [Casesnoves, 2018] is a type of Nonlinear Optimization that combines separation of variables method with stages of Graphical Optimization [Casesnoves, 2016], [Interior Graphical-Optimization Methods were created by Francisco Casesnoves on 3<sup>rd</sup> November 2018, while he was preparing

his Doctoral Thesis defence. First implementation of algorithms and computational-verification of simulations were carried out in the morning of April 1<sup>st</sup>, 2020].

In optimization with objective functions based on nonlinear systems of equations, or multiobjective-parameters constraints and other conditions, the task is rather difficult. Specifically this occurs in Physics and Engineering nonlinear optimization problems. Large-scale amount of empirical data for algorithms/models implementation have to be adapted/fitted to models that involve a high number of equations, nonlinear many of them, constraints added. Stochastic Optimization methods are used to save time and computational effort when the amount of data is large. In these cases, it is not necessary to work with all the numerical volume available.

Approximations and final refinements for mathematical models are usually performed with inverse methods. Statistical-estimations/Approximations and errors testing are obtained from all alternative formulation available. In previous contributions, Graphical Optimization was presented and applied for engineering mathematical modelling, materials erosion models [Refs-9, 12,22,27], and physics of deformable solids dynamics.

However, Graphical Optimization involves the objective function visualization in 2D-3D imaging-processing software. This implies that multiparameter formulas initially cannot be easily set for the 3D Graphical Optimization, unless a choice of 2 or 3 variables is done among several ones. From this apparent difficulty, a mathematical optimization and software engineering method for an objective function of high number of variables arose and is presented. It is defined as Interior-Graphical Optimization Method [Casesnoves, 2018]. This observed fact implied also that some complementary approaches to the theory of Nonlinear Equations systems could be done.

Furthermore, in this line, it is proven for optimization that the solution for multiobjective optimization problems is not unique in general in [Refs-8, 9,13]. This occurs in nonlinear systems equations. The method was intended to be proven and set, at first, on simple equations at Electronics Physics field, namely BCS algorithms [Refs-8, 9,13]. Therefore, brief-direct applications in electronics field for superconductors isotope-effect and critical temperature are also presented.

In summary, this briefing-review shows an advanced contribution for the Interior Nonlinear Optimization Method previously presented in [Refs-8, 9,12,13]. Mathematical and computational base is explained/proven for the classical superconductor Hg Type I. The scheme of the method is shown, with a sharp proof in applications at this electronics field. A clear demonstration that Nonlinear Systems do not have unique solution in general constitutes a supplementary mathematical frame of this paper can be found at [Refs-8, 9,13].

#### 4.1 Mathematical Methods and Algorithms and Matrix Algebra

Linear systems are included in this study as a nonlinear ones with exclusively unitarian power and without nonlinear operations among parameters. Consider the multiobjective problem with constraints,

CLASSICAL MULTI OBJECTIVE OPTIMIZATION ALGORITHM,  
(SIMPLEST):

*minimize,*  
 $f(\vec{X}) = F[f_1(\vec{x}_1), f_2(\vec{x}_2), \dots, f_N(\vec{x}_N),]$   
*subject to,*  
 $\vec{a}_1 \leq \vec{x}_1 \leq \vec{b}_1;$   
 $\vec{a}_2 \leq \vec{x}_2 \leq \vec{b}_2;$   
 $\dots$   
 $\vec{a}_N \leq \vec{x}_N \leq \vec{b}_N;$   
*Further linear and nonlinear constraints can be added;*

(3)

Where,

$f(X)$ : Vectorial principal function.  $X$  is a vector of sub-functions.  
 $f(x_i)$ : Sub-function component of principal function vector or matrix, every  $x_i$  is a vector. Such as,  
 $F(X) = [f(x_1), \dots, f(x_N)]$   $i=1 \dots N$ .  
 $a_i$ : Lower boundary constant. ( $i = 1 \dots N$ ).  
 $b_i$ : Upper boundary constant. ( $i = 1 \dots N$ ).  
 $N$ : Number of matrix functions.

This (3) is an equation of several variables that has not, in general, unique solution. If the objective function becomes an [i] number of nonlinear functions. Hence,

INTERIOR OPTIMIZATION MULTI OBJECTIVE ALGORITHM,  
(SIMPLEST APPLIED):

*for*  $i = 1 \dots N$ ,  
*minimize,*  
 $f(x_i) = F[x_{i1}, x_{i2}, \dots, x_N]$   
*subject to,*  
 $\vec{a}_{i1} \leq \vec{x}_{i1} \leq \vec{b}_{i1};$   
 $\vec{a}_{i2} \leq \vec{x}_{i2} \leq \vec{b}_{i2};$   
 $\dots$   
 $\vec{a}_{iN} \leq \vec{x}_{iN} \leq \vec{b}_{iN};$   
*Further linear and nonlinear constraints can be added;*

(4)

Where,

$f(X)$ : Vectorial principal function.  $X$  is a vector of sub-functions.  
 $f(x_i)$ : Sub-function component of principal function vector or matrix, every  $x_i$  is a variable-vector. Such as,  
 $f(X) = F[x_{i1}, x_{i2}, \dots, x_{iN}]$   $i = 1 \dots N$ . The is a sub-function of  $N$  variables, everyone is a vector.  
 $a_i$ : Lower boundary constant. ( $i = 1 \dots N$ ).  
 $b_i$ : Upper boundary constant. ( $i = 1 \dots N$ ).  
 $N$ : Number of matrix functions.

Therefore, it is a system of nonlinear equations functions with several variables, [Refs-9, 12, 13, 26], that in general case do not have to be equal in number to the parameters. If there are terms with operations among parameters, and roots, the unique solution is even more difficult to be find out. Optimization algorithms and software can find usually a local minimum, semi-global minimum, or a local minimum according to constraints. A classical method is Monte-Carlo programs, such as GEANT type, classically used in IMRT-IMPT radiotherapy, although there are options for Monte-Carlo and Quasi-Monte-Carlo software available. Jacobian and classical Newton-Raphson methods are, for example, used to find an approximate solution. Number of methods to find solution/approximate solutions for a system of nonlinear equations are extent, and it is not the specific focus of this contribution. Monte-Carlo method can be considered methods to find solution/approximate solutions for a system of nonlinear equations are extent. Monte-Carlo method can be considered good, because the program usually, taking continuous random values, search for an optimal solution of variables, no matter how many they are.

Genetic Algorithms constitutes an stochastic method that has proven be very useful and precise nowadays.

Given this algorithm, the Graphical and Interior Optimization Methods can be applied starting for grouping variables step by step. The technique is an extrapolation of the classical partial equations method of separation of variables. That is,

INTERIOR OPTIMIZATION MULTI OBJECTIVE ALGORITHM,  
(SIMPLEST TECHNIQUE):

*if optimization stage is,*  
*minimize,*  
 $f(\vec{X}) = f[x_1, x_2, \dots, x_N]$   
*by using similar partial differential method*  
*of separation of variables, for instance,*  
*if it is at principal function, a product, such as,*  
 $x = x_1 \bullet x_2,$   
*it is grouped for a 3D axis imaging – processing as,*  
 $x_{1s} = x_1 \bullet x_2,$   
*and so one;*

(5)

Where,

$f(X)$ : Vectorial principal function.  $X$  is a vector of one sub-function.

$f(x_i)$ : Sub-function component of principal function vector or matrix, every  $x_i$  is a variable-vector.

$N$ : Number of matrix functions.

$x_i$ : A variable-vector.  $S$  is the number of sub-functions.

Or just the same parameters-grouping for sums, exponentials, etc. Thus, the technique begins with a 3D graph of two selected parameters, at Z axis the objective function. The optimal/desired values are fixed at that graph. Those fixed values are taken for the subsequent 3D graph that involves the following two parameters, and so on.

What is done in mathematical concepts, is to apply the partial differential equations classical separation of variables method. With separation of variables, it is possible to optimize all the parameters in subsequent stages of 3D graphical optimization plots. At every plot, it is selected the desirable local, global, or semi-local minimum for the variable of convenience.

In such a way that the initial Graphical Optimization begins with 3 variables, namely, first, second and objective function. An optimal value is determined. The following stage one parameter with two variables is decomposed, and it is taken the optimal values, and so on.

Therefore, it is easy to prove, through the multi-selection of local and approximate minima at Graphical Optimization sets, that in general the multiobjective solution for a system of nonlinear equations is not unique. In other words, it is demonstrated from 3D visualization and separation of variables, this classical mathematical assertion.

Number of graphs required depend on the number of variables of the nonlinear system of equations. The determination of optimal values not necessarily have to be minima. Optimal values taken depend of the engineering requirements for laboratory optimization, devices manufacturing, experimental plan, or similar tasks. The advantage is that the software engineering gives a fast tool to find necessary data immediately with short time consuming.

## 4.2 Optimization Algorithms for Superconductor Isotope Effect

In this section a brief summary of Superconductivity towards the Transition Equation and the Isotope Effect in

BCS Theory is presented. The Superconductivity Theory framework is rather extent and with large mathematical background. It involves Quantum Theory, Molecular Chemistry, Materials Physics and other science and engineering branches. All these areas converge together in Superconductors theory and applications. Which is useful to prove Interior Optimization Method are the simple equations of Transition-Temperature-Critical and Isotope Effect [Refs-9, 37]. The classical-simple Critical Temperature Equation for superconductors reads,

ISOTYPE EFFECT MULTIOBJECTIVE ALGORITHM,  
(SIMPLEST FORMULATION):  
for  $i = 1, \dots, N$ , number of element isotopes,  
 $[M_i]^\alpha T_{Ci} - K_i \cong 0$ ,  
for  $i = 1, \dots, N$ ;  
Further linear and nonlinear modifications/constraints can be added; (6)

Where,

K: Sub-function component of principal function vector or matrix, every  $x_i$  is a vector. Such as,  
 $M_i$  = Atomic mass of every isotope. AMU.  
 $\alpha$ : Isotope effect constant power parameter. Adimensional.  
Tci: Critical Temperature of every isotope. Kelvin.  
i: Isotope number for everyone of them.

From the stage when the solid reaches critical temperature, the superconductivity effect begins. TC varies for every isotope element within a defined mass element, although not excessively in magnitude.

This equation, although simple, remains useful today. It was taken to illustrate Interior Optimization Method in simple way. The evolution of this equation, for example, [Refs-7, 2], involves extent mathematical background and mathematical-physics theory. It is sufficient to prove the Interior Optimization Method with this classical equation. Just note that taking decimal or Neperian logarithms the equation (6) can be linearized for setting graphics related to different isotopes with corresponding atomic proper mass. To set the simplest nonlinear system of equations, for Hg Isotope Effect Interior Optimization, the algorithm selected with 100 equations reads,

ISOTYPE EFFECT MULTIOBJECTIVE  
OBJECTIVE FUNCTION ALGORITHM,  
CHEBYSHEV L1 NORM,  
(SIMPLEST FORMULATION):  
for  $i = 1, \dots, N$ , number of element isotopes,  
everyone with proper  $T_C$ ,  
minimize,  
 $\| [M_i]^\alpha T_{Ci} - K_i \|_{L_1}$ ;  
subject to,  
 $a \leq M_i \leq a_1$ ;  
 $b \leq T_{Ci} \leq b_1$ ;  
 $c \leq K_i \leq c_1$ ;  
 $d \leq \alpha \leq d_1$ ;  
NOTE: At imaging - processing it is also  
implemented Objective Function as,  
 $OF = [M_i]^\alpha T_{Ci} - K_i$ ,  
Further linear and nonlinear modifications/constraints can be added; (7)

Where,

$K_i$ : Isotope Effect constant for every isotope.  
 $M_i$  = Atomic mass of every isotope. AMU.  
 $\alpha$ : Isotope effect constant power parameter. Adimensional.  
Tci: Critical Temperature of every isotope. Kelvin.  
i: Isotope number for everyone of them.  
a,  $a_1$ : Lower and upper boundary constant for  $M_i$ . (i = 1, ..., N). AMU.

b,  $b_1$ : Lower and upper boundary constant for Tci. (i = 1, ..., N). Kelvin.  
c,  $c_1$ : Lower and upper boundary constant for every  $K_i$  at implemented interval. (i = 1, ..., N).  
d,  $d_1$ : Lower and upper boundary constant for every  $\alpha_i$  at implemented interval. (i = 1, ..., N). Adimensional.  
N: Number of isotopes.  
 $\| \cdot \|_{L_1}$ : Chevyshev norm.

Where i is the corresponding number within the range of simulations. For example, in range of simulations for Hg, M [Refs-7, 10-11] is,

$$M \in [199.5, 203.4] \quad (8)$$

In the same way, range of constraints can be seen in axes ranges of Figures 9-13. Therefore, with Equations 1-7, a nonlinear system of equations is set. The variables are to get optimized. The method is Interior-Graphical Optimization, that is proven accurate and useful for [Refs-8, 9]. It was taken Hg superconductivity values from literature [Refs-7, 10-11]. Extrapolation to large and complicated Electronic Physics equations, Electronics, or any type of system can be guessed from this application.

#### 4.3 Software Engineering Dataset

The software developed for this contribution had some easy parts and not a few programming difficulties to adapt the programs on Chebyshev L1 norm for objective function, Equations 1-7. Additional complications were the algebra changes in the subroutines to get functional the program for surface Graphical Optimization visualization. This requires mathematical changes-background.

The software was developed in GNU-Octave and Matlab and is almost equivalent for Freemat also. These numerical data are all for this contribution. In previous contributions, higher values were taken for high-accuracy. Graphical Optimization programs were designed for double precision, since were based on engineering software of extent number of previous publications.

To check complementarily the numerical results, both Fortran and F# subroutines in optimization were used. While Fortran proved to match the Graphical Optimization results, F# showed restrictions and obviously, limits that discarded this type of language for accurate results in nonlinear optimization. None of these F# numerical data were included in publication.

**Table 5:** Dataset implemented in programs for Hg Interior Optimization. That is a classical experimental foundation of Hg superconductivity, [From Refs-7, 10 -11, experimental]. Dataset is at software patterns in intervals

INTERIOR OPTIMIZATION SOFTWARE DATASET Hg ISOTYPE EFFECT	
[From Refs-7, 10 -11, experimental data]	
PARAMETER	MAGNITUDE INTERVAL PROGRAMMING IMPLEMENTED
M, Isotope Atomic Mass (AMU)	[199.5, 203.4] AMU
Experimental Alpha	[0.30, 0.60]
Experimental Critical Temperature Tc, (K)	[4.146, 4.185] K
K constant calculation from experimental data	[50.00, 60.00]
The Figures show imaging processing patterns with/without L1 Chevyshev norm for explicit clarity to prove the global minima	

#### 4.4 Computational Graphical-Interior Optimization Results

The results are shown in Tables and Graphics. Numerical results matches values in the literature for natural Hg. However, alpha value is lower than the classical magnitude of 0.5, from [Refs-7, 10-11].

Residuals can be considered acceptable, although not of high-precision accuracy. The time consuming for designing program is extremely short. The time for selecting optimal values is also very short with the Matlab graphical cursor. In engineering practice, this is a significant advantage that gives many options for fast on-site superconductivity data management at laboratory. Results confirm useful utility of Equations 1-7.

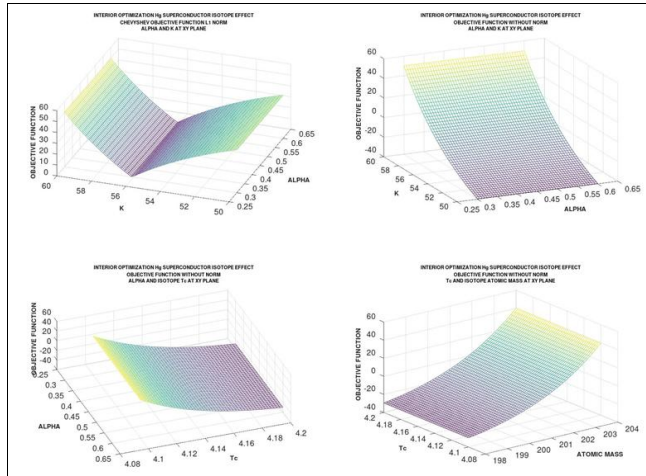


**Fig 9:** GNU-Octave multiple imaging-processing for Hg advanced Interior-Graphical optimization. It was graphically determined the optimal K value and the power magnitude for constant  $\alpha$ . First image is got with L1 Chevyshev norm. The others are set with simple OF. The first image shows intersection line of global minima line for alpha and K at XY plane. The others set at XY plane the alpha-Tc and Tc-Atomic-Mass numerical functions. At  $Z=0$ , can be sharply seen the global minima proof. Running time si about 2-4 seconds

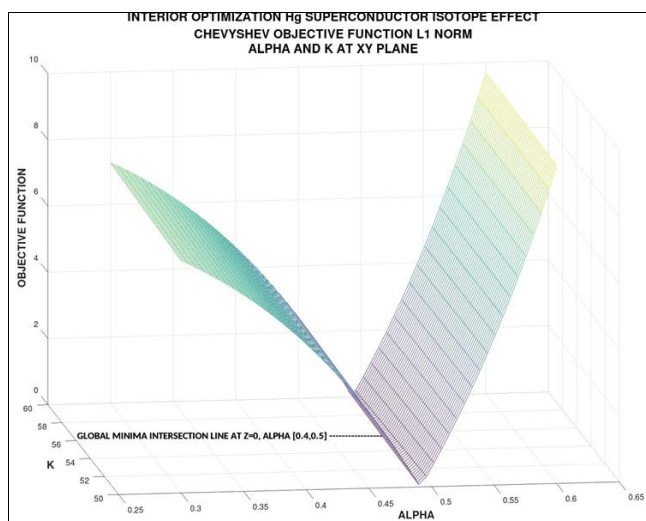


**Fig 10:** GNU-Octave imaging-processing for Hg advanced Interior-Graphical optimization. It was graphically determined the optimal K value and the power magnitude for constant  $\alpha$ , inset marked global minima line. Image is got with L1 Chevyshev norm. It shows intersection line of global minima line for alpha and K at XY plane. Running time si about 2 seconds

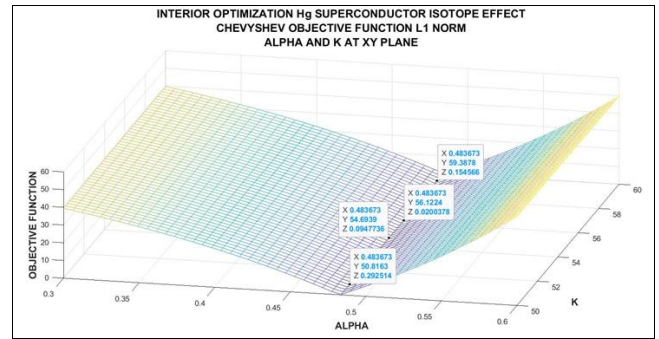


**Fig 11:** Matlab imaging-processing for Hg advanced Interior-Graphical optimization. It was graphically determined the optimal K value and the power magnitude for constant  $\alpha$ , inset marked global minima line. Image is got with L1 Chevyshev norm. It shows intersection line of global minima line for alpha and K at XY plane. Dataset, inset, is used for numerical results graphical calculations. Running time si about 2 seconds

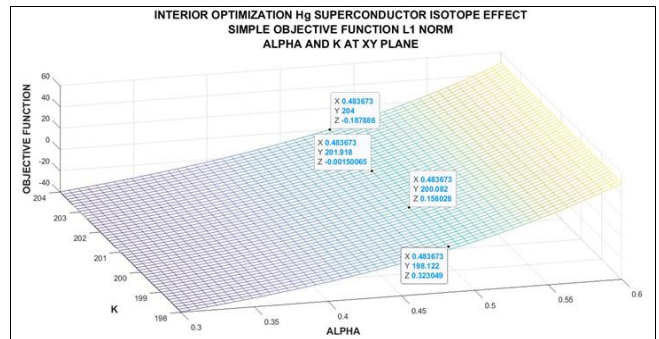


**Fig 12:** Matlab imaging-processing for Hg advanced Interior-Graphical optimization. It was graphically determined the optimal K value and the power magnitude for constant  $\alpha$ , inset marked global minima line. Image is got without L1 Chevyshev norm. It shows of global minima points-line for alpha and K at XY plane. Dataset, inset, is used for numerical results graphical calculations. Running time si about 2 seconds. At GNU-Octave graphics, the usual magnitude of alpha was around [0.490]

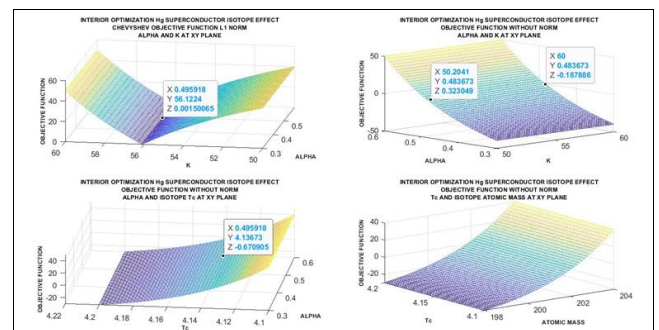


**Fig 13:** Matlab multiimaging-processing for Hg advanced Interior-Graphical optimization. It was graphically determined the optimal K value and the power magnitude for constant  $\alpha$ , inset marked global minima line. First image is got with L1 Chevyshev norm, the others without. It is shown of global minima points-line for alpha and K at XY plane, alpha and Tc, and Tc and Atomic Mass. Dataset, inset, is used for numerical results graphical calculations. Running time si about 1-3 seconds. OF residuals at Z axis are low

**Table 6:** 2D-3D Interior-Graphical optimal results got from imaging-processing series. Results are slightly lower than publications for Hg, [Refs-7, 10-11]

INTERIOR OPTIMIZATION NUMERICAL RESULTS Hg ISOTOPE EFFECT [From Refs-7, 10 -11, experimental data]	
PARAMETER	OPTIMAL INTERVAL FOR ALL ISOTOPE AMU (Data obtained from Interior-Graphical Optimization)
M, Isotope Atomic Mass (AMU)	[201.0,201.0] AMU (For any other OF parameter)
Experimental Alpha	[0.480,0.495] (For any other OF parameter)
Experimental Critical Temperature Tc, (K)	[4.125, 4.140] K (For any other OF parameter)
K constant calculation from experimental data	[56.30,56.40] (For any other OF parameter)

The Figures show imaging processing patterns with/without L1 Chevyshev norm for explicit clarity to prove the global minima

## 5. Discussion and Conclusions

The objectives of the research were to improve the Molecular Effect Model for HTSC Cuprates by using 2D-3D Interior and Graphical Optimization. The MEM model built was based on an initial 3-degree polynomial fit taking Critical Temperatures related to HTSC Cuprates (Hg-Ba-Ca-Cu-O) Molecular Masses. Second objective was to determine Carnot Factors 2D-3D imaging-processing dataset for up-to-date current cuprates.

Results comprise a low-error MEM improved for Cuprates. 2D-3D abs errors (K);  $[0 \leq \text{Abs Error} \leq 8]$  (K). Average 2D-3D Error= 4.0633 K; (Figures 1-4). Although some errors are high, the statistical mode is low, then average error results be about 4 K. All errors are proven in 2D-3D imaging series, with corresponding numerical results. The Carnot Factor calculations are shown in 2D-3D charts for different Operating Temperature magnitudes. As a result from the software methods used, a series of new programs were got for software advances in Graphical and Interior Optimization. A review of Isotope Effect classical model was included from previous contributions [Refs-8, 1-13, book 9].

Results of improved software and imaging-processing for Hg Isotope Effect, Interior Optimization show advances both in 3D Interior Optimization and numerical results. The improved-review proves programming method, precision that matches literature database, namely [Refs-7, 10-11], and demonstrates the efficacious software implemented and method. The numerical magnitude precision for Hg SC Type I alpha constant is improved at Table 6, lower than literature publications, [Refs-7, 10-11]

Therefore, MEM presented shows errors  $[0 \leq \text{Abs Error} \leq 8]$  (K). These can be considered an advance from previous contributions. Efficacious utility of this MEM predictions for a range of isotopes are detailed in Tables 3-4.

In summary, Molecular Effect Model improvements were got with Tc predictions for possible proportion variants in molecule isotopes composition. Secondly Carnot Factor for cuprates was optimized and presented in 2D-3D chart series. An improved-review of Hg Isotope Effect was included and Electronics Physics applications were explained.

## 6. Scientific Ethics Standards

Automatic Artificial Intelligence software was NOT used for Author's original software-engineering in this article. If

AI is used at any Author's publication, it is referred. All images of this study are new and contain improved programming, [Casesnoves, May 7th, 2024] from previous publications [Refs-8, 1-13]. All mathematical algorithms are reviewed and improved. Methods from were begun be created by Dr Francisco Casesnoves in 3<sup>rd</sup> November 2007, and Interior Optimization Methods in 2019. This article has previous papers information, from [Refs-8, 9], whose inclusion is essential to make the contribution understandable. This study was carried out, and their contents are done according to the International Scientific Community and European Union Technology and Science Ethics [Refs-9, 45-47]. For example: 'European Textbook on Ethics in Research'. European Commission, Directorate-General for Research. Unit L3. Governance and Ethics. European Research Area. Science and Society. EUR 24452 EN. Also based on 'The European Code of Conduct for Research Integrity'. Revised Edition. ALLEA. 2017. This research was completely done by the author, the computational-software, calculations, images, mathematical propositions and statements, reference citations, and text is original for the author. When a mathematical statement, algorithm, proposition or theorem is presented, demonstration is always included. When a formula is presented, all parameters are detailed or referred. If any results inconsistency is found after publication, it is clarified in subsequent contributions. Note: The numerical value of Hg SC alpha constant has been found better from [Refs-8, 9], it was a slight magnitude inconsistency. When a citation such as [Casesnoves, 'year'] is set, it is exclusively to clarify intellectual property at current times, without intention to brag. The article is exclusively scientific, without any commercial, institutional, academic, any religious, religious-similar, no companies-influences, non-scientific theories, personal opinions, political ideas, or other economical influences. When anything is taken from a source, it is adequately recognized, or put an mber in a remark.

## 7. Superconductors Cuprates and Hg References

1. Wesche R. High-temperature superconductors: Materials, properties, and applications. Springer, 1998.
2. Narlikar A. Superconductors. Oxford, 2014.
3. Poole C, Alt. Superconductivity. Elsevier. 2017, 2007.
4. Bussmann-Holder A, Keller H, Bianconi A. High-Tc Copper Oxide Superconductors and Related Novel Materials. Springer. 2017, 2017
5. Plakida N. High-Temperature Cuprate Superconductors Experiment, Theory, and Applications. In Springer Series in Sol-id-State Sciences; Springer: Berlin/Heidelberg, 2010.
6. Khare N. Handbook of High-Temperature Superconductor; Marcel Dekker: New York, NY, 2003.
7. Sarrao J, Nault R. Basic research needs for superconductivity. Report on the Basic Energy Sciences Workshop on Superconductivity, 2006.
8. Thomas H, Alt. Superconducting transmission lines - Sustainable electric energy transfer with higher public acceptance? Renewable and Sustainable Energy Reviews. Elsevier. 2016; 55:59-72.
9. Lebrun P, Alt. Cryogenics for particle accelerators and detectors. European Organization for Nuclear Research. Laboratory for Particle Physics. Divisional Report. CERN LHC/2002-11, 2002.

10. Reynolds C, Serin B, Nesbitt B. The Isotope Effect in Superconductivity. I. Mercury. The Isotope Effect in Superconductivity, Mercury. *Physical Review*, November 1951; 84(4).
11. Serin B, Reynolds C, Nesbitt B. Mass Dependence of the Superconducting Transition Temperature of Mercury. *Letters to Editor. Phys. Rev.* 1950; 80:761.

## 8. Author's Superconductors Main Publications

### References

1. Casesnoves F. Interior Optimization Methods with Electronics Applications. *Int. J. Sci. Res. Sci. Eng. Technol.* 2020; 7:428-436. [CrossRef]
2. Casesnoves F. Advanced Interior Optimization Methods with Electronics Applications. *Int. J. Sci. Res. Sci. Eng. Technol.* 2020; 7:97-110. [CrossRef]
3. Casesnoves F. Multiobjective Interior Optimization Computational Methods for Electronics BCS Superconductivity. *Int. J. Sci. Res. Comput. Sci. Eng. Inf. Technol.* 2020; 6:280-293. [CrossRef]
4. Casesnoves F. Superconducting materials critical temperature models designed with 3D interior Optimization methods. *Scientific talk and Proceedings Conference. PON AQUI Conferencia.* 2023; 4.
5. Casesnoves F. Genetic Algorithms for Interior Comparative Optimization of Standard BCS Parameters in Selected Superconductors and High-Temperature Superconductors. *Standards MDPI.* 2022; 2:430-448. Doi: <https://doi.org/10.3390/standards2030029>
6. Casesnoves F. Mathematical-Computational Optimization Methods on Primary Molecular Effect Model for Selected High Temperature Superconductors with Electronics Physics Applications. *International Journal of Scientific Research in Computer Science, Engineering and Information Technology (IJSRCSEIT)*, March-April 2022; 8(2):159-167. ISSN: 2456-3307. Doi: <https://doi.org/10.32628/CSEIT228220>
7. Casesnoves F. Genetic Algorithms Optimization for High Temperature Superconductors Sn Class Molecular Effect Model with Electronics Applications. *International Journal on Recent Technologies in Mechanical and Electrical Engineering.* 2022; 9(3). ISSN: 2349-7947
8. Casesnoves F. Genetic Algorithms Molecular Effect Model Optimization for High Temperature Superconductors Tin and Thallium Classes. *Recent Trends in Programming Languages.* 2022; 9(3):1-16. Doi: 10.37591/RTPL
9. Casesnoves F. Interior Optimization Methods with electronics Applications Examples. *Eliva Press.* 2023.
10. Casesnoves F. Interior Dual Optimization Software Engineering with Applications in BCS Electronics Superconductivity. *Asian Journal of Mathematical Sciences*, Jul-Sep 2020; 4(3). ISSN: 2581-3463
11. Casesnoves F. Superconductors Molecular Effect Model Fundamentals and Review of Isotope Effect with 3D Graphical-Mathematical Interior Optimization. *J Eng App Sci Technol.* 2024; 6(8):1-10. ISSN: 2634-8853
12. Casesnoves F. Superconducting Multifunctional Transmission Line Fundamentals. *International Journal on Recent Technologies in Mechanical and Electrical Engineering*, September 2022; 9(3). ISSN: 2349-7947. <http://www.ijrmee.org>
13. Casesnoves F. Interior Optimization Methods with Electronics Applications. *International Journal of Scientific Research in Science, Engineering and Technology (IJSRSET)*, May-June 2020; 7(3):428-436. Online ISSN: 2394-4099, Print ISSN: 2395-1990, Doi: <https://doi.org/10.32628/IJSRSET207377>. Journal URL: <http://ijsrset.com/IJSRSET207377>

## 9. General References

1. Vora AM. Modified Transition Temperature Equation for Superconductors. *Chin. Phys. Lett.* 2008; 25:2162. [CrossRef]
2. Casesnoves F. Interior Optimization Methods with Electronics Applications. *Int. J. Sci. Res. Sci. Eng. Technol.* 2020; 7:428-436. [CrossRef]
3. Casesnoves F. Advanced Interior Optimization Methods with Electronics Applications. *Int. J. Sci. Res. Sci. Eng. Technol.* 2020; 7:97-110. [CrossRef]
4. Casesnoves F. Multiobjective Interior Optimization Computational Methods for Electronics BCS Superconductivity. *Int. J. Sci. Res. Comput. Sci. Eng. Inf. Technol.* 2020; 6:280-293. [CrossRef]
5. Alexandrev AS. *Theory of Superconductivity, from Weak to Strong Coupling*. Series in Condensed Matter Physics; Institute of Physics Publishing: Philadelphia, PA, USA, 2003.
6. Buschow K. *Magnetic & Superconducting Materials*, 2nd ed.; Elsevier: Amsterdam, The Netherlands, 2003.
7. Seidel P. *Applied Superconductivity*; Wiley-VCH: Hoboken, NJ, USA. 2015; 1-2.
8. Drechsler S, Mishonov T. *High-TC Superconductors and Related Materials Material Science, Fundamental Properties, and Some Future Electronic Applications*; Springer Science Media: Berlin/Heidelberg, Germany, 1998.
9. Kazufumi I, Bangti J. *Inverse Problems, Tikhonov Theory and Algorithms*; Series on Applied Mathematics; World Scientific: Singapore. 2015; 22.
10. Casesnoves F. Mathematical Models and Optimization of Erosion and Corrosion. *Ph.D. Thesis*, Taltech University, Tallinn, Estonia, December 14, 2018. ISSN: 25856898
11. Casesnoves F. *Die Numerische Reuleaux-Methode Rechnerische und Dynamische Grundlagen mit Anwendungen (Erster Teil)*; *Scienza Scripts*: Chisinau, Moldova, 2019. ISBN: 139786200895608/106200895600
12. Casesnoves F. Primary Modelling for Electromagnetic Waves Transmission in Extreme Weather Conditions. *Int. J. Innov. Res. Sci. Eng. Technol.* 2018; 7:10294-10300. [CrossRef]
13. Casesnoves F. The Numerical Reuleaux Method, a Computational and Dynamical Base with Applications. First Part; Lambert Academic Publishing: Saarland, Germany, 2019. ISBN: 103659917478
14. Darwin C. *The Origin of Species*; Barnes & Noble Classics: New York, NY, USA, 2004.
15. Haupt R, Haupt S. *Practical Genetic Algorithms*, 2nd ed.; Wiley: New York, NY, USA, 2004.
16. Abramowitz M, Stegun IA. *Handbook of Mathematical Functions*; U.S. Government Printing Office: Champaign, IL, USA. 1964; 55.
17. Casesnoves F, Suzenkov A. Mathematical Models in Biotribology with 2D-3D Erosion Integral-Differential

Model and Computational-Optimization/Simulation Programming. *Int. J. Sci. Res. Comput. Sci. Eng. Inf. Technol.* 2017; 2:329-356. ISSN: 24563307

18. Casesnoves F, Antonov M, Kulou Piss. Mathematical models for erosion and corrosion in power plants. A review of applicable modelling optimization techniques. IEEE Xplore database and will be cross referred in SCOPUS. In Proceedings of the RUTCON2016 Power Engineering Conference, Riga, Latvia, October 13, 2016.

19. Casesnoves F. 2D computational-numerical hardness comparison between Fe-based hardfaces with WC-Co reinforcements for Integral-Differential modelling. *Key Eng. Mater. J.* 2018; 762:330-338; ISSN: 16629795 [CrossRef]

20. Casesnoves F, Surzhenkov A. Inverse methods for computational simulations and optimization of erosion models in power plants. In Proceedings of the RUTCON2017 Power Engineering Conference, Riga, Latvia, December 5, 2017. [CrossRef]

21. Casesnoves F. Computational Simulations of Vertebral Body for Optimal Instrumentation Design. *J. Med. Devices.* 2012; 6:021014. [CrossRef]

22. Casesnoves F. Large-Scale Matlab Optimization Toolbox (MOT) Computing Methods in Radiotherapy Inverse Treatment Planning. In High Performance Computing Meeting; Nottingham University: Nottingham, UK, 2007.

23. Casesnoves F. A Monte-Carlo Optimization method for the movement analysis of pseudo-rigid bodies. In Proceedings of the 10th SIAM Conference in Geometric Design and Computing, San Antonio, TX, USA. Contributed Talk, November 4-8, 2007.

24. Casesnoves F. Applied Inverse Methods for Deformable Solid Dynamics/Kinematics in Numerical Reuleaux Method (NRM). *Int. J. Numer. Methods Appl.* 2013; 9:109-131.

25. Casesnoves F. Nonlinear comparative optimization for biomaterials wear in artificial implants technology. In Proceedings of the Applied Chemistry and Materials Science RTU2018 Conference Proceedings, Rajasthan Technical University, Kota, India, March 17-18, 2018.

26. Allison J, Amako K, Apotolakis J, Araujo H, Dubois PA, Asai M, *et al.* Geant4 Developments and Applications. *IEEE Trans. Nucl. Sci.* 2006; 53:270-278. [CrossRef]

27. Batic M, Hoff G, Pia MG, Saracco P, Weidenspointner G. The Geant4 Simulation Toolkit. *IEEE Nucl. Sci. Symp. Med. Imaging Conf. Seoul.* 2013; 60:2934-2957.

28. Luenberger GD. Linear and Nonlinear Programming, 4th ed.; Springer: Berlin/Heidelberg, Germany, 2008.

29. Huang X. Does the isotope effect of mercury support the BCS theory?, 2011. arXiv 2011, arXiv:1102.1467.

30. Hummel RE. Electronic Properties of Materials; Springer: New York, NY, USA, 2011.

31. Kasap F, Capper P. (Eds.). Springer Handbook of Electronic and Photonic Materials, 4th ed.; Springer: Berlin/Heidelberg, Germany, 2000. [CrossRef]

32. Kessel W. On a General Formula for the Transition Temperature of Superconductors. *Naturforschung.* 1974; 29a:445-451. [CrossRef]

33. Kulo P, Casesnoves F, Simson T, Tarbe R. Prediction of abrasive impact wear of composite hardfacings. *Solid State Phenomena.* In Proceedings of 26th International Baltic Conference on Materials Engineering; Trans Tech Publications: Bäch, Switzerland. 2017; 267:201-206. [CrossRef]

34. Luiz A. Superconductivity-Theory and Applications; In TechOpen: London, UK, 2010. ISBN: 9789533071510

35. Reynolds CA, Serin B, Nesbitt LB. The Isotope Effect in Superconductivity. I. Mercury. *Phys. Rev.* 1951; 84:691. [CrossRef]

36. Seri B, Reynolds CA, Nesbitt LB. Mass Dependence of the Superconducting Transition Temperature of Mercury. *Letters to Editor. Phys. Rev.* 1950; 80:761. [CrossRef]

37. Todinov M. Reliability and Risk Models; Wiley: New York, NY, USA, 2005.

38. Vidyasagar M. Nonlinear Systems Analysis, 2nd ed.; Prentice Hall: Hoboken, NJ, USA, 1993.

39. Wesche R. Chapter 50. High-Temperature Superconductors. In Springer Handbook of Electronic and Photonic Materials; Springer: Berlin/Heidelberg, Germany, 2017.

40. Parinov I. Microstructure and Properties of High-Temperature Superconductors, 2nd ed.; Springer: Berlin/Heidelberg, Germany, 2017.

41. Fossheim K, Sudbø A. Superconductivity Physics and Applications; Wiley: New York, NY, USA, 2004.

42. Wang Y. Fundamental Elements of Applied Superconductivity in Electrical Engineering; Wiley: New York, NY, USA, 2013.

43. European Textbook on Ethics in Research. European Commission, Directorate-General for Research. Unit L3. Governance and Ethics. European Research Area. Science and Society. EUR 24452 EN, 2021. Available online: <https://op.europa.eu/en/publicationdetail/-/publication/12567a07-6beb-4998-95cd-8bca103fcf43> (accessed on 28 June 2021).

44. ALLEA. The European Code of Conduct for Research Integrity, Revised ed.; ALLEA: Bern, Switzerland, 2017.

45. Swedish Research Council. Good Research Practice; Swedish Research Council: Stockholm, Sweden, 2017. ISBN: 978-91-7307-354-7

46. Sarrao J, Nault R. Basic research needs for superconductivity. Report on the Basic Energy Sciences Workshop on Superconductivity, 2006.